ROYAL SOCIETY
OF CHEMISTRY

Check for updates

Protein conformational ensembles in function: roles and mechanisms

Ruth Nussinov, [ID] *[abc] Yonglan Liu,[c] Wengang Zhang[c] and Hyunbum Jang [ID] [ac]

The *sequence-structure-function* paradigm has dominated twentieth century molecular biology. The paradigm tacitly stipulated that for each sequence there exists a single, well-organized protein structure. Yet, to sustain cell life, function requires (i) that there be more than a single structure, (ii) that there be switching between the structures, and (iii) that the structures be incompletely organized. These fundamental tenets called for an updated *sequence-conformational ensemble-function* paradigm. The powerful energy landscape idea, which is the foundation of modernized molecular biology, imported the conformational ensemble framework from physics and chemistry. This framework embraces the recognition that proteins are dynamic and are always interconverting between conformational states with varying energies. The more stable the conformation the more populated it is. The changes in the populations of the states are required for cell life. As an example, *in vivo*, under physiological conditions, wild type kinases commonly populate their more stable "closed", inactive, conformations. However, there are minor populations of the "open", ligand-free states. Upon their stabilization, *e.g.*, by high affinity interactions or mutations, their ensembles shift to occupy the active states. Here we discuss the role of conformational propensities in function. We provide multiple examples of diverse systems, including protein kinases, lipid kinases, and Ras GTPases, discuss diverse conformational mechanisms, and provide a broad outlook on protein ensembles in the cell. We propose that the number of molecules in the active state (inactive for repressors), determine protein function, and that the dynamic, relative conformational propensities, rather than the rigid structures, are the hallmark of cell life.

Introduction

The energy landscape concept[1–4] inspired experimental and computational approaches to characterize biomolecular ensembles that are now bearing functional insight.[5–8] The landscape concept underscored the importance of proper physicochemical description of biological molecules—not as single structures but as ensembles with dynamic distributions that change with changes in the environment.[9–24] While the classical sequence-*single structure*-function dogma has been enormously useful and influential in driving the relevance of structure in biology over multiple decades, it did not portray the non-linear propagation of information which is responsible for life.[5] Different from the free energy landscape outlook, the single structure paradigm that prevailed for scores of years failed in embracing multiple states, thus in capturing

biological actions, since its underlying premise has been unable to describe biological macromolecular dynamics. This is important since X-ray structures capture only snapshots, which are unable to explain exactly how function is executed. Adhering to a single shape leads to (i) attempting to explain molecular mechanisms by arguing that binding of incompatible shapes forces "pushing" molecules to change their shapes, rather than recognizing that binding involves selection of compatible shapes among the many available with subsequent minor conformational changes for optimization, which relieve incurring energetic conflicts.[25,26] It also fails in (ii) identifying the preferred activation pathway in *e.g.*, kinases, which requires not only a catalogue of the conformational states but their occupancies.[27–33] And importantly, consequently it is unable to (iii) capture allosteric mechanisms.[34–42] In enzymatic reactions,[23,41,43–45] conformational dynamic amplifies the heterogeneity of the transition state.[46] This suggests that the classical view of catalysis as a single tight optimized transition-state structure lowering the activation energy may also need to be updated to a transition state surface. In this population landscape view, rather than a single well-defined transition-state structure, enzymes can bind efficiently with a transition-state ensemble.

[a] *Computational Structural Biology Section, Frederick National Laboratory for Cancer Research, Frederick, MD 21702, USA. E-mail: NussinoR@mail.nih.gov*

[b] *Department of Human Molecular Genetics and Biochemistry, Sackler School of Medicine, Tel Aviv University, Tel Aviv 69978, Israel*

[c] *Cancer Innovation Laboratory, National Cancer Institute, Frederick, MD 21702, USA*

Physical and chemical principles underlie the fundamental functional processes harnessed by living systems in their diverse environments. In proteins and RNA, these include not only the conformational ensembles, but the kinetic barriers separating them, which function may need to overcome.[47–50] Under normal physiological conditions, proteins largely populate their inactive conformations with the ensembles harboring only a minor population of the active state. Binding of effectors, or the membrane, can stabilize the active states, increasing the probabilities of barrier crossing. Oncogenic mutations similarly increase the relative stability of the active *versus* inactive conformations, mimicking this physicochemical principle.[38,51–54] Thus, binding, whether noncovalent by effectors or covalent as in the case of mutations, posttranslational modifications, and protein family members with similar, albeit not identical sequences, modify the free energy landscape, driving the ensemble over the barriers, tipping the stability scales, and accomplishing a bistable switch.

Unquestionably, structural biology is essential for understanding biological processes. Equally so is the premise that conformational ensembles underlie all protein functions.[23,55–58] The challenging aim facing the community is to elucidate the functions, especially how they are executed at the basic conformational level, and the mechanistic underpinnings of their signaling pathways. A conformational view is essential for in-depth comprehension of how proteins work and how they are regulated in the cell. Often single structures are harnessed to depict proteins and their interactions to explain observations, and the databases collect them. Undoubtedly, the mammoth task of assembling cellular, biochemical, protein–protein interaction, clinical, and high-resolution structural data results in an extremely useful overall picture; however, it still falls short. On their own these databases still cannot decipher the relationship between distinct isoforms and their preferred signaling pathways; nor are they able to explain mutational, or isoform, consequences, or the root causes of oncogenic signaling trends which correlate with specific cancers. They are critical; but insufficient. By harnessing dynamic populations, a conformational view of the data can bridge structural and cellular data and make these connections. Their foundation is the notion that biomolecules are not static sculptures, and their relative populations determine their functional states. Within this framework, our pioneering dynamic free energy landscape and redistribution of the population concepts, which were validated by numerous experiments, serve as guiding principles for deciphering function and dysfunction.[59–62]

The protein sequence-*conformational ensemble*-function paradigm was inspired by the realization that even living things must conform to the laws of physics, including the laws of motion and structural chemistry. At the same time, conformational principles are insufficient to explain protein actions *in vivo*. The cell is complex.[63,64] Molecular concentrations are influenced by cell types and states, thus chromatin accessibility. Ensembles are also influenced by feedback loops. Through the actions of negative feedback loops, which often wield phosphatases, such as phosphatase and tensin homolog (PTEN) or dual specificity phosphatase 6 (DUSP6), tumor suppressors which can stymie active conformations and curb signaling.[65–69] The ensembles are also impacted by the

inherent liquefied droplets in the dynamic spatial structure of the cell, which extends from small complexes and assemblies to micrometer scales and coordinates cellular behavior.[70–74]

Below, we first discuss allostery,[40,75–83] a hallmark of the functional role of conformational ensembles, followed by examples drawn from kinases and small GTPases. The references above provide more. These examples fit into the classical description of conformational ensembles, *i.e.*, those generated by (almost) the same sequence, including single point mutations. We then expand our discussion to ensembles generated by isoforms and homologs belonging to the same family. In our outlook, isoforms and homologs with similar sequences occupy the same states, albeit with different propensities, thus favoring different ligands. Examples include cyclin-dependent kinase (CDK) family homologs CDK1, CDK2 and CDK4,[84] and Ras. K-Ras4A favors Raf-1, K-Ras4B favors B-Raf.[85] Along these lines, Rap1A, a GTPase highly homologous to K-Ras4B (Fig. 1), activates B-Raf, but not Raf-1 due to the lower affinity of the Raf-1 Ras binding domain (RBD) to the Rap1A catalytic domain, and the consequent failure of Raf-1 activation, which is not the case for B-Raf.[86]

Allostery is a hallmark of function. If no protein conformations, no allostery, and no function

The free energy landscape is forceful since it can capture the mapping of all possible conformations that the molecule can populate. The lower the energy the higher the population. Mapping on a Cartesian coordinate system is both simple and powerful. With only small differences in energies among the states, the ensemble of (sub)states tend to lie within the native, lowest energy basin (Fig. 2A). A minor change in the stabilities of these near-energy states can easily flip an inactive state to an active one. The more stabilized is the active state *versus* the inactive state the more potent will be the bistable switch of the energy scales toward it and the stronger the resulting emitted signal. The rate of the switch is a function of the relative occupancies of the states on the energy mapping. The switch from the inactive to the active (and *vice versa*) is driven by allostery.[59,87,88] Allostery can be triggered by noncovalent or covalent binding events,[88–112] leading to conformational and dynamic changes,[36,41,94,95,113–120] by inciting local energetic frustration, or conflicts.[25,121–123] Conformational changes relieving the frustration propagate in the structure, shifting the ensemble from the inactive toward the stable, minimally frustrated active state (Fig. 2B). Thus, rather than the classical two active/inactive states captured by crystallography, there are multiple conformations in the ensemble with multiple possible propagation pathways. The favored route proceeds through the one involving lower kinetic barriers.[89,124–128] Allosteric propagation pathways pre-exist in the ensemble, with preferred pathways required for functional population shift. In two (or multi) domains proteins joined by long, disordered linkers, the probability of propagation *via* the linker is relatively low. The disordered state harbors multiple conformations.[129–135] It is

© 2023 The Author(s). Published by the Royal Society of Chemistry
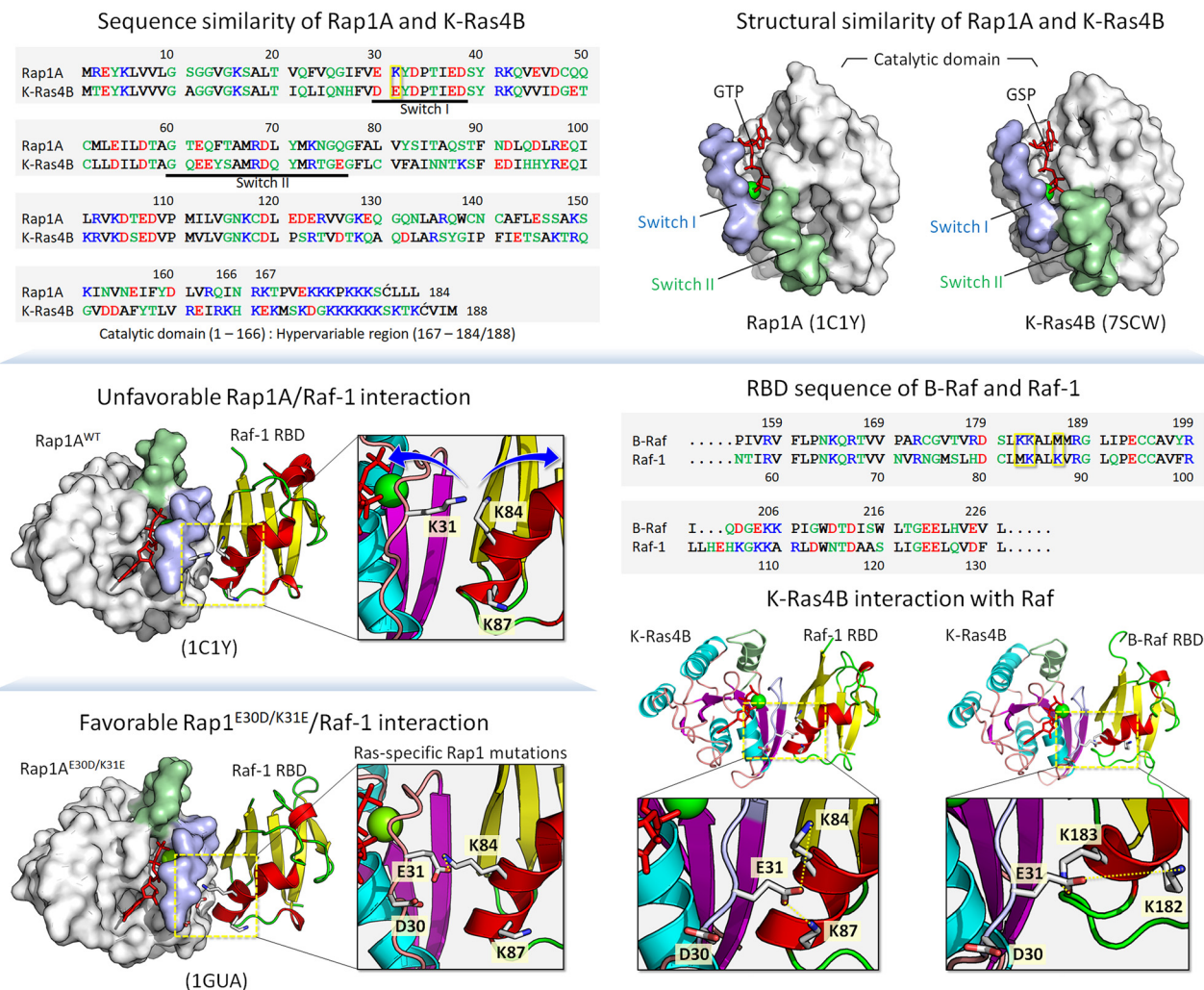
RSC Chem. Biol., 2023, **4**, 850–864 | 851

Fig. 1 Sequence alignment and side-by-side comparison of the catalytic domain structures of Rap1A and K-Ras4B showing similarity (*top panels*). In the sequence, hydrophobic, polar/glycine, positively charged, and negatively charged residues are colored black, green, blue, and red, respectively. The yellow box at position 31 in the sequence indicates a key residue involved in the Raf RBD interaction. The crystal structure of the Rap1A catalytic domain interacting with the Raf-1 RBD shows an unfavorable interaction due to electrostatic repulsion between Lys31 of Rap1A and Lys84 of the Raf-1 RBD (*middle left panel*). Ras-specific mutation E30D/K31E of Rap1A restores interaction with Raf-1 RBD (*bottom left panel*). RBD sequences of B-Raf and Raf-1 and highlighting key residues in the yellow boxes that are involved in the GTPase interaction (*middle right panel*). Small GTPases interact with Raf through their catalytic domains, forming a strong backbone β-sheet interface with the Raf RBD. In addition to the backbone interaction, a strong salt bridge interaction contributes to the stability of the complex, as shown by the model structures of K-Ras4B interacting with the Raf-1 and B-Raf RBDs (*bottom right panels*). The example shows that Glu31 of K-Ras4B can form salt bridges with Lys84 and Lys87 of the Raf-1 RBD and Lys182 and Lys183 of the B-Raf RBD.

characterized by its remarkable conformational flexibility and structural plasticity[136] and its prevalence in the proteome,[137–140] testifying to its usefulness. In the absence of specific stable interactions, there are likely no preferred propagation pathways. Raf's activation can serve as an example. Even though Ras binding initiates allosteric propagation in Raf's RBD, with a long, disordered linker, the signal is unlikely to be responsible for activation of Raf's kinase domain. Instead, it is more likely that the high affinity interactions shift the Raf ensemble from the inactive to the active state, liberating its autoinhibition.[141]

Allostery is how proteins are regulated. Autoinhibition and activation are allosteric events. Allosteric events can be impacted by concentration (since higher concentration implies higher chances for intermolecular contacts), can take place *via*

coordination by ions, by interactions with signaling lipids, small molecule ligands, proteins, nucleic acids, and water molecules. Because allosteric propagation involves alterations of interactions at the atomic/residue level, a short-range allosteric signal is expected to be stronger. Through the occupancy of the relevant states, statistical mechanics relates the free-energy landscapes to the atomic level properties of molecules, and the macroscopic behavior of a population of molecules,[2,9,21,142,143] where the occupancy of the states is a function of their relative energies. For enzymes, the catalytic reaction rate relates to the population of each state on a multidimensional energy landscape and the probability of reacting from that state.[23] Below we provide a range of examples of the roles and mechanisms played by protein conformational ensembles in function.
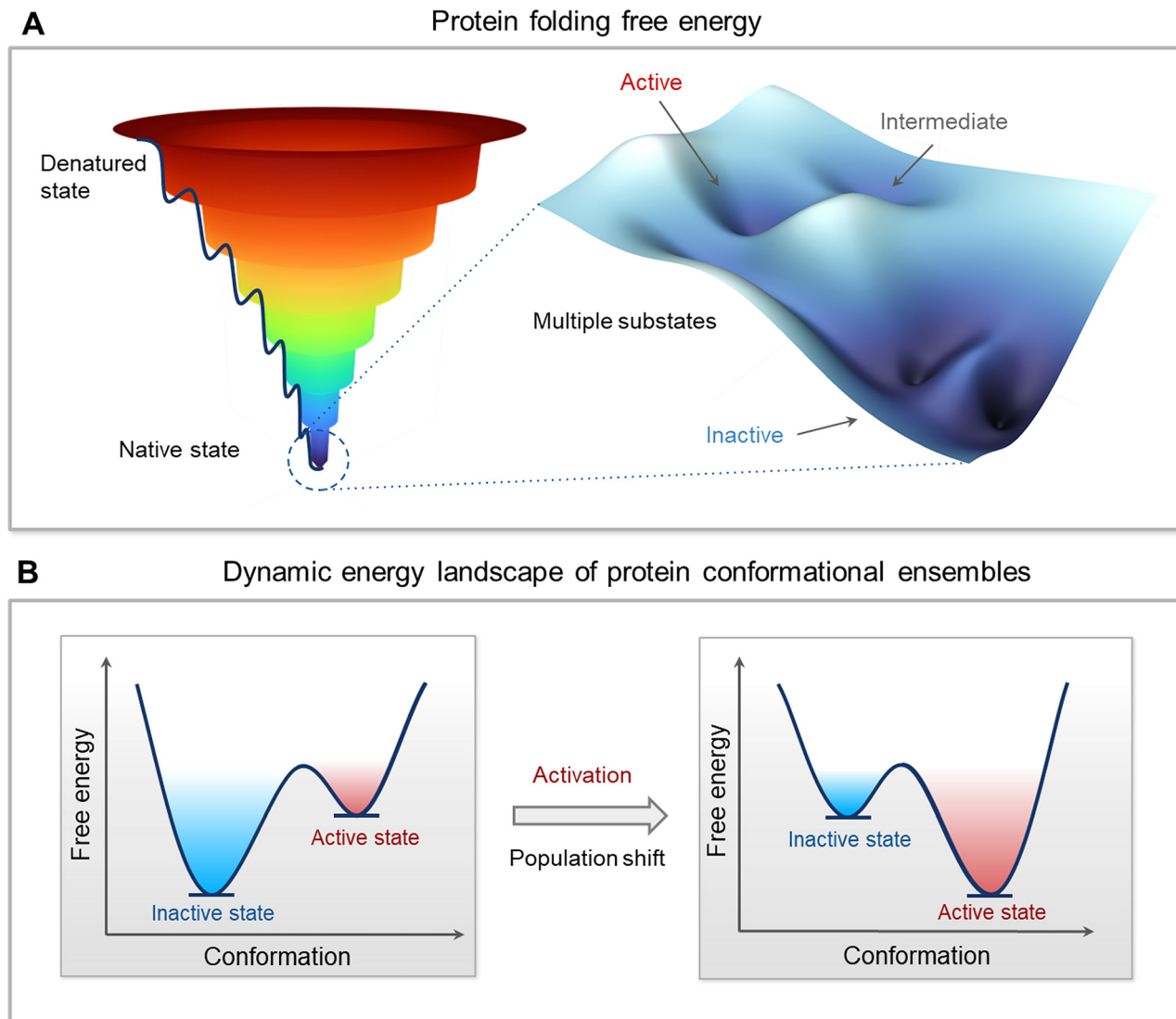
Fig. 2 Multidimensional free energy landscape and conformational dynamics of protein. (A) Protein folding free energy landscape on a Cartesian coordinate system using a funnel-like shape with local valleys and peaks representing the vast ensembles of protein conformations. The depth or height of a point within the funnel corresponds to the free energy of a conformation, with deeper valleys indicating lower energy states and higher likelihood of occupancy. The native state is characterized by the lowest-energy valley at the bottom of the funnel, where the protein's functional conformations are concentrated. Within this native state, the landscape is populated with multiple substates, such as inactive states typically having the lowest energy, active states with slightly elevated energy, and intermediate states that can act as transition configurations. Subtle changes in the energy landscape at the bottom of the funnel, around the native state, can have profound effects on a protein's function and ability to interact with other molecules. The color gradient, ranging from deep blue at the bottom (indicative of lower energy) to red at the top (indicative of higher energy), visually encodes the probability of state occupancy and reflects the stability of conformations. (B) Dynamic energy landscape and how external factors such as genetic mutations, post-translational modifications like phosphorylation, and interactions with ligands or other proteins can alter the landscape. These alterations induce shifts in the population distribution of protein conformations, effectively transitioning proteins from a predominantly inactive state to an active state or *vice versa*. The figure emphasizes the dynamic nature of proteins and how their function is intrinsically tied to their conformational flexibility and adaptability within the cellular environment.

The conformational ensemble of c-Abl autoinhibition and activation is controlled by a myristoyl lipid moiety, a posttranslational modification

Abl, the key kinase in leukemia, is an allosterically regulated non-receptor tyrosine kinase.[144–153] There are two alternatively spliced Abl isoforms,[147] 1a and 1b (Fig. 3A). The N-terminus of the 19-residue longer 1b, but not of 1a, harbors a covalently connected myristoyl. Apart from this distinction, the isoforms have the same structural elements, the SH3, SH2, and kinase domains. In the autoinhibited conformation, the SH2 and SH3 domains latch onto the back of the kinase domain (Fig. 3B), with the N-terminal disordered region further contributing to Abl autoinhibition[147,154] *via* its proline-rich (Cap^{PxxP}) and C-terminal caps (Cap^{C}).[146] Sites to which posttranslational modification moieties are attached are typically disordered. The
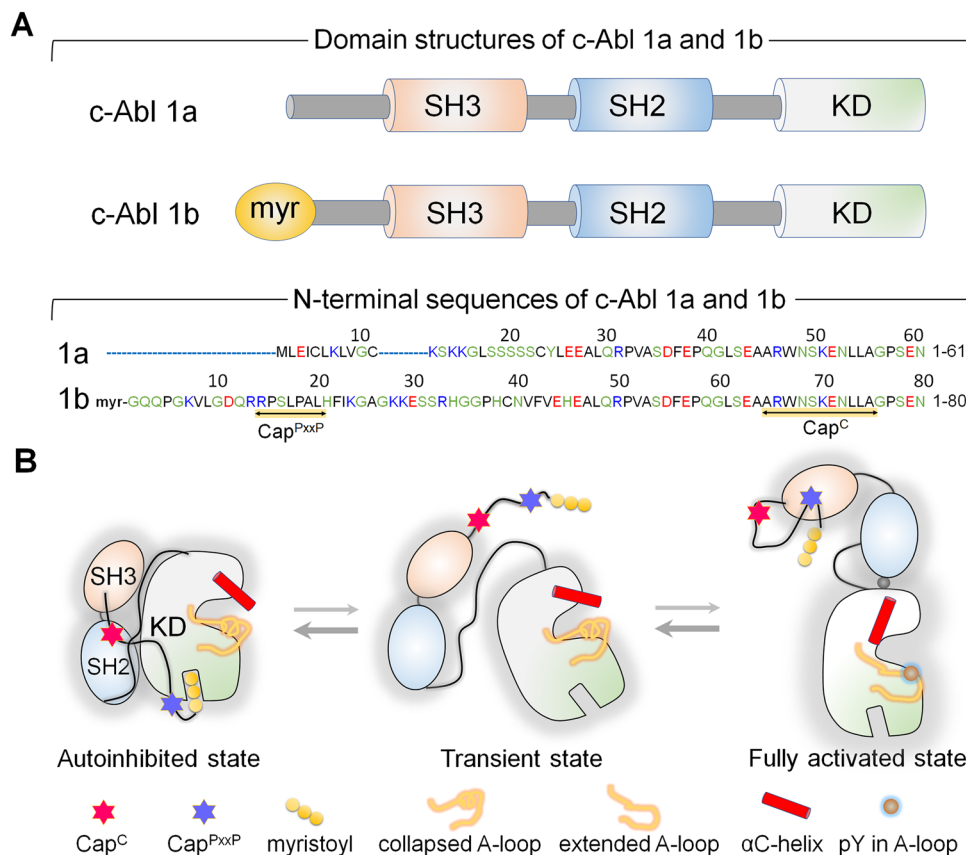
Fig. 3 (A) The c-Abl protein exists in two isoforms: 1a and 1b. Both isoforms share three common domains: SH3, SH2, and kinase domains. A myristoyl group connects the N-terminus of the 1b isoform, which is not present in 1a. The N-terminal region of the 1b isoform is 19 residues longer compared to the 1a isoform. Both isoforms possess a Cap^C region, while only the 1b isoform contains a Cap^{PxxP} motif. (B) In the autoinhibited state of c-Abl 1b, the SH3 and SH2 domains dock onto the back of the kinase domain, and the myristoyl group inserts into a pocket within the C-lobe of the kinase domain. The Cap^C region interacts with the SH2 domain, lashing the SH2–SH3 module to the kinase domain. The myristoyl group acts as a switch for Abl's autoinhibition and activation. Upon release of the myristoyl group, the SH2–SH3 module dissociates from the kinase domain. The SH2 domain undergoes reorientation and translocation, relocating to interact with the top region of the N-lobe of the kinase domain, fully activating Abl. When autoinhibition is released, the canonical polyproline type II (PPII)-binding site of the SH3 domain of the c-Abl 1b isoform becomes exposed, potentially enabling optimal interaction with the Cap^{PxxP} motif. Abbreviation: KD, kinase domain.

myristoyl moiety acts as the switch between the autoinhibited and activated Abl. Binding of the myristoyl to the C-lobe pocket stabilizes Abl's autoinhibited conformation; its release triggers a conformational change which promotes the release of the SH2–SH3 domains. The released SH2 domain undergoes reorientation and translocation, inducing a transition toward a catalysis-favored conformation. The αC-helix shifts from the OUT to the IN conformation stabilizing the interacting P-loop/αC,[146] the IN αC-helix, the R-spine, and the compact ATP-binding space.

Abl provides an example of how, through optimized positioning and atomistic contacts, a posttranslational modification toggles a conformational ensemble of a kinase driving its functional transition.

The conformations of the stronger K-Ras4B G12V oncogenic mutation visit the active state more frequently than those of the weaker G12D mutation

The conformational ensemble of a protein is heterogeneous, and the distributions of the same conformations by different

mutants differ. That is, the mutations bias the ensemble differently, depending on how stabilizing (or destabilizing) the mutation is. Features of conformations that are stabilized by strong activating mutations resemble those of the active state. A strong mutation more forcefully biases the conformational ensemble toward the catalytic state, which is connected to the clinical phenotypes, by creating more favorable interactions. K-Ras is a good example.

Active K-Ras GTPase activates its effectors which then activate major signaling cascades in the cell, including MAPK and PI3K/AKT/PDK1/mTOR (Fig. 4). Both pathways are key actors in aggressively stimulating cell proliferation, survival, and invasion in cancer. The mutations point to variable tumorigenic outcome, including response to chemotherapy.[155–159] K-Ras4B strong activating mutations act by blocking GTP hydrolysis. The strongest involve substitutions of G12, G13, and Q61. Weaker mutations disable nucleotide exchange, GDP by GTP.[160,161] Among the G12 mutations, G12D is the most common, especially in pancreatic cancer, where it is present in approximately 35% of people diagnosed with the disease, and G12V is the most aggressive and chemotherapy resistant.
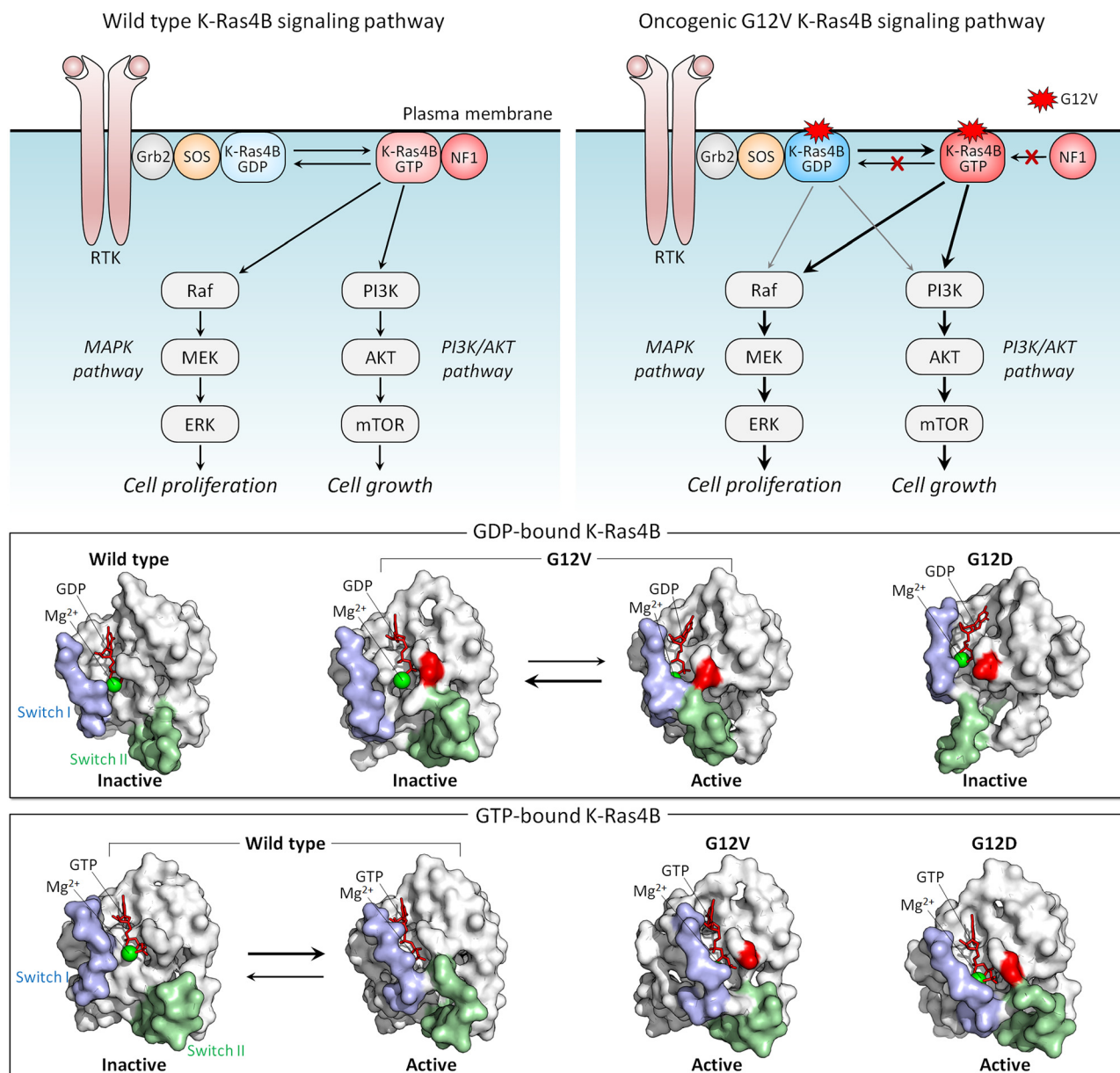
© 2023 The Author(s). Published by the Royal Society of Chemistry

Fig. 4 K-Ras4B signaling pathway. K-Ras4B is activated by SOS, a nucleotide exchange factor (GEF), *via* the GDP-to-GTP exchange and deactivated by NF1, a GTPase-activating protein (GAP) *via* the GTP-to-GDP hydrolysis (*top left panel*). Oncogenic driver mutations at the position 12, such as G12D, G12C, and G12V, impair the GAP-mediated hydrolysis and maintain Ras in a constitutively active GTP-bound state (*top right panel*). In the MAPK pathway, active GTP-bound K-Ras4B proteins recruit Raf to the plasma membrane and lead to Raf activation through dimerization of kinase domains. Active Raf dimers lead to the activation of a series of the MAPK kinases, resulting in cell proliferation. In the PI3K/AKT pathway, K-Ras4B recruits PI3K to the plasma membrane, leading to the production of the signaling lipid PIP_3, which recruits AKT to the membrane, followed by activation by PDK1 and mTORC2. Active AKT is involved in the activation of mTORC1, leading to cell growth. Active-like, GDP-bound K-Ras4B with oncogenic G12V mutation can activate MAPK and PI3K/AKT pathways. The GDP-bound K-Ras4B (*middle panel*) and GTP-bound K-Ras4B (*bottom panel*) structures. In surface representation, two distinct conformations correspond to the inactive and active-like structures for K-Ras4B^{G12V}-GDP, and the inactive-like and active structures for K-Ras4B^{WT}-GTP. Both K-Ras4B^{G12V}-GDP and K-Ras4B^{WT}-GTP exhibit the open and closed Switch I and Switch II conformations. The open and closed switch regions represent K-Ras4B in the inactive and active states, respectively. Abbreviation: RTK, receptor tyrosine kinase; Grb2, growth factor receptor-bound protein 2; SOS, Son of sevenless; NF1, neurofibromin 1, MAPK, mitogen-activated protein kinase; MEK, mitogen-activated protein kinase kinase; ERK, extracellular signal-regulated kinase; PI3K, phosphoinositide 3-kinase; AKT, protein kinase B; mTOR, mammalian target of rapamycin.

NMR, crystallography, and computations were used to explore why G12V mutations are more aggressive than G12D.[162]

The conformational behavior of K-Ras4B oncogenic mutants G12D and G12V differs[34] (Fig. 4). While both favor an active-like state resembling GTP-bound K-Ras, the extent varies, due to the distinct atomic interactions formed by valine and the Switch II region in the GDP-bound K-Ras4B as compared to aspartic acid. These have not been captured in the crystal structures, where crystal contacts favor alternate stabilized Switch I region, but were observed by NMR and molecular dynamics simulations. We

expect that this mechanism applies broadly, clarifying the differential strengths of mutations: stronger activating mutations favor more strongly the active state.[163,164] To put it in terms of dynamic fluctuating ensembles, conformations favored by strong mutations visit the active state more frequently than weaker mutations do. In the case of K-Ras4B, which is not an enzyme, the conformation of the active state is the one that preferentially binds its effectors, such as Raf and PI3K.[165,166] Visiting the active state more frequently is important for function since this results in the protein spending more time in the active, here oncogenic, state.

PI3K: conformational transitions for phosphorylation at the membrane

PI3Kα (PI3K below) lipid kinase phosphorylates signaling lipid PIP_2 to PIP_3 (Fig. 5A). The ensuing signaling cascade proceeds through the major PI3K/AKT/mTOR pathway.[167] AKT and mTOR are protein kinases that phosphorylate innumerable substrates, thereby regulating cell growth, proliferation, differentiation, migration, mobility, and apoptosis.[168,169] Their activating mutations drive cancer and neurodevelopmental disorders.[170–172]
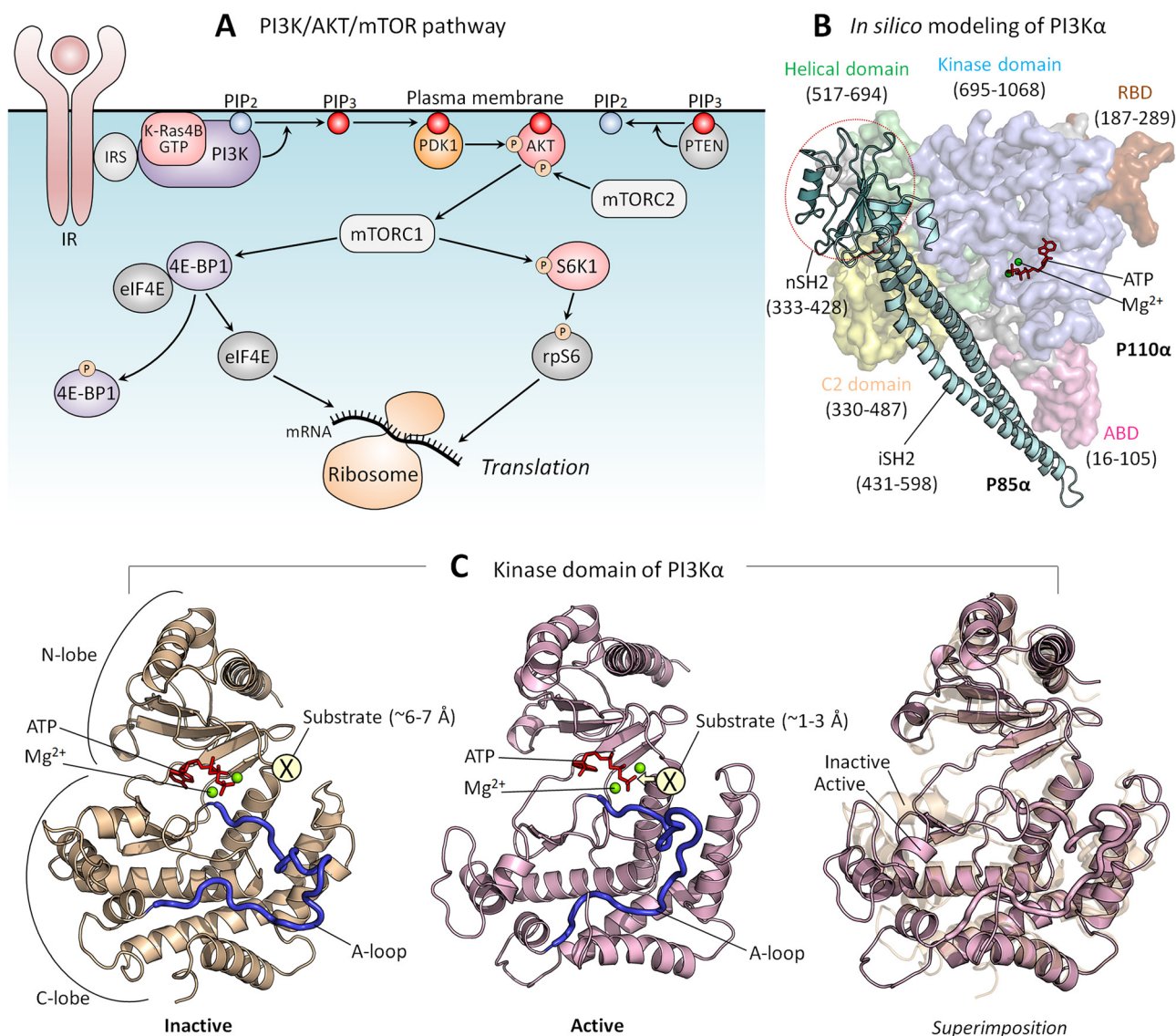

Fig. 5 (A) In the PI3K/AKT/mTOR pathway, the lipid kinase, PI3K is activated by IR and IRS. PI3K phosphorylates PIP_2 to PIP_3, and PTEN dephosphorylates PIP_3 back to PIP_2. PDK1 and mTORC2 phosphorylate and activate PIP_3-bound AKT, leading to mTORC1 activation. Active mTORC1 phosphorylates 4E-BP1 and S6K1. Phosphorylated 4E-BP1 releases eIF4B, which initiates mRNA translation at the ribosome. Phosphorylated S6K1 phosphorylates rpS6, also resulting in the initiation of mRNA translation. (B) An *in silico* model structure shows PI3Kα in an inactive state derived from the crystal structure (PDB: 4OVV). (C) The kinase domain structure of PI3Kα in the inactive (*left panel*) and active (*middle panel*) states and the superimposition of both (*right panel*). The active kinase domain structure was obtained from our previous studies.[167] In the inactive state, the substrate, the inositol head of PIP_2, is located ∼6–7 Å from the γ-phosphate of the ATP. In the active state, the substrate is located ∼1–3 Å from the γ-phosphate of the ATP. Abbreviation: IR, insulin receptor; IRS, insulin receptor substrate; PI3K, phosphoinositide 3-kinase; PIP_2, phosphatidylinositol 4,5-bisphosphate; PIP_3, phosphatidylinositol 3,4,5-trisphosphate; PDK1, phosphoinositide-dependent protein kinase 1; AKT, protein kinase B; mTORC1/2, mammalian target of rapamycin complex 1/2; 4E-BP1, eukaryotic translation initiation factor 4E (eIF4E)-binding protein 1: S6K1, ribosomal S6 kinase 1; rpS6, ribosomal protein S6.

PI3K's action is opposed by PTEN tumor suppressor which dephosphorylates PIP_3 to PIP_2. PI3K is a functional heterodimer consisting of the catalytic $p110\alpha$ and the regulatory $p85\alpha$ (Fig. 5B), which under physiological conditions is involved in inhibition of the $p110\alpha$ catalytic activity.[173] The landmark crystal structure with the soaked PIP_2 captured its binding site.[174] Since it is away from ATP, and the nSH2 domain attached to the $p110\alpha$ subunit, it portrayed PI3K in its inactive state. *In vivo*, activation involves binding of the p85 nSH2 domain to phosphorylated C-terminal of activated receptor tyrosine kinases (RTKs), such as the insulin receptor, and active K-Ras. Calmodulin can also activate PI3K.[175–177] The nSH2–RTK interaction disrupts the interactions of the nSH2 with the helical domain of the catalytic subunit, and of the iSH2 domain of p85 with the C2 domain of p110. These conformational changes result in relocation of the ABD of the catalytic subunit, and in interaction of the kinase domain with the membrane, which is promoted by Ras.[53] Ras binding increases the PI3K residence time at the membrane, fostering PIP_2 binding at the active site. Thus, RTKs allosterically activate PI3Kα; however, merging their action with Ras accomplishes full activation.[141] At the same time, exactly how these actions, which are far away from the catalytic site, relate to PI3K activation has been unclear. It was also unclear how nSH2 interaction with the RTKs and the conformational changes that it stimulates lead to these actions and activation.

Transfer of a phosphoryl group from a donor to a receptor requires a distance of 1–3 Å[174] (Fig. 5C). The crystal structure of the inactive PI3K points to $\sim$6–7 Å between the γ-phosphate of the ATP and the PIP_2. This conundrum has been resolved by data showing that the interaction of the phosphorylated, activated RTK allosterically triggers conformational transitions, culminating in reduced distance and in a reoriented, exposed kinase domain on the membrane.[167] nSH2 release removes conformational constraints and leads to formation of new stabilizing interactions. The C-lobe of the kinase domain, where the PIP_2 binds to a positively charged residue patch, moves away from the C2 domain, the C2/helical/C-lobe angle increases, and the distance between the C2 domain and the C-lobe of the kinase domain increases as well. Thus, through multiple conformational transitions emerging from allosteric energetic conflicts incurred by the binding of the nSH2 domain with the C-terminal of the insulin receptor, these conformational changes result in the kinase domain surface becoming fully accessible for interaction with the membrane.

Affinity and shift of the ensemble are a key mechanism for conformational transition in Raf's activation by Ras at the membrane

In the cell, the ensemble of Raf monomers can populate several states. These include (i) Ras-free open conformations, (ii) autoinhibited closed Raf conformations, which are inactive, and (iii) active Ras-bound conformations.[141] In the absence of active Ras, the most highly populated conformation is the closed autoinhibited state (Fig. 6). It is the most stable.[178] In this conformation, the surface of the kinase domain which serves for dimerization is occluded. There is only a minor population of the unstable open, Ras-free state. In the presence of active, GTP-bound Ras at the membrane, the RBD of Raf interacts with Ras with high affinity (measured in solution to be in the nanomolar range),[179–181] as does Raf's cysteine-rich domain (CRD) with the membrane.[182–184] CRD binding is stabilized by its positively charged membrane insertion loop.[182,185] The Ras—RBD-CRD organization at the membrane tamps down the Ras—RBD fluctuations, increasing Raf's cooperative stabilization at the membrane. In the absence of active Ras molecules, Raf mostly populates a closed autoinhibited state, where the access to the kinase domain is hindered by other Raf domains/segments.

The high affinity Ras—RBDs and CRD—membrane interactions stabilize the open, Ras-bound state, leading to a population shift toward this conformation largely from the less stable, open Ras-free ensemble, which is likely separated from the Ras-bound state by low kinetic barriers. The shift impacts the relative populations, thus equilibrium between the Ras-free open state and the closed state, which is restored mostly by a shift of the autoinhibited state (Fig. 6). The resulting high population of the open, stabilized Ras-bound state, with the exposed surface of the kinase domain, enables its dimerization. Depending on the location in different Raf isoforms, with 14-3-3 involvement, phosphorylation may weaken or promote the autoinhibition.[186–194]

Thus, data and theory suggest that allostery, *via* a Ras-promoted conformational change, does not play a role in neither PI3Kα nor Raf activation.[195] Significantly, in agreement with this, no activating mutations that can replace Ras are located in the RBDs, of neither Raf nor PI3K.

In the literature it is often noted that active Ras anchored at the plasma membrane "recruits" Raf. Such "recruitment" terminology is used quite frequently. We clarify that recruitment invariably implies a high affinity interaction that stabilize the conformation, thus a shift of the population toward the recruited state.

Splicing, and different gene isoforms, may share ensembles, although with different propensities

The Ras superfamily is diverse, with multiple members. Among them, three major genes encode Ras, *HRAS*, *NRAS*, and *KRAS*.[196] Their sequences are highly similar, but not identical. Their mutational frequencies differ, with *KRAS* most frequently mutated, and *HRAS* and *NRAS* expression appearing insufficient to promote oncogenesis when mutated.[197] Their protein products, K-Ras, H-Ras and N-Ras, differ primarily in their C-terminals, and in the attached combination of lipid posttranslational modifications. There are also minor differences in their catalytic domains. Their structures are highly similar as
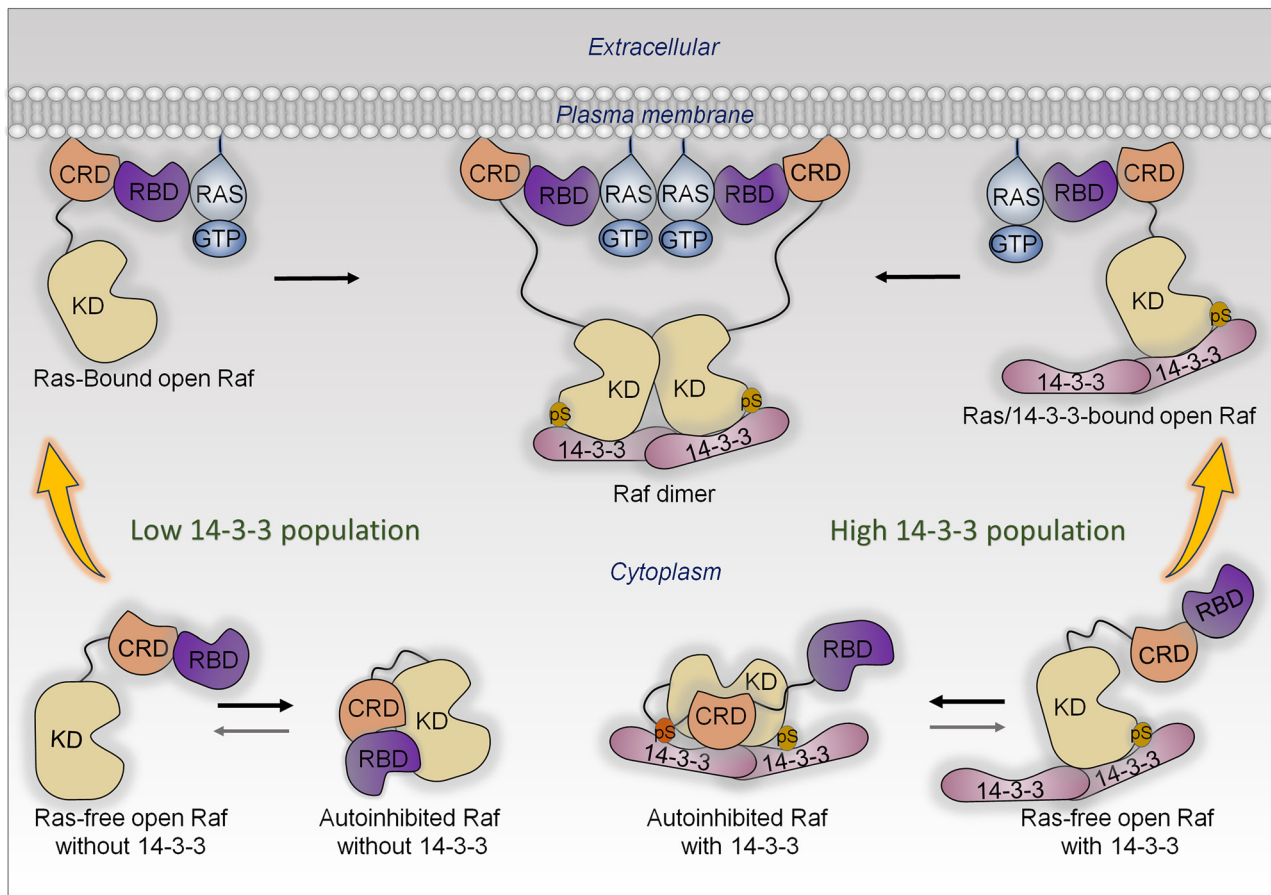
© 2023 The Author(s). Published by the Royal Society of Chemistry

RSC Chem. Biol., 2023, **4**, 850–864 | **857**

Fig. 6 All Raf kinases share three conserved regions (CRs); CR1 involves the tandem Ras-binding domain (RBD) and cysteine-rich domain (CRD), CR2 contains the Ser/Thr rich region at the flexible linker, and CR3 is the kinase domain (KD). In the cytosol, Raf can exist in two autoinhibited states in the presence and absence of 14-3-3. When 14-3-3 concentration is low, Raf populates the closed, autoinhibited state without 14-3-3. In this state, the CRD and RBD dock onto the kinase domain. This closed state is most stable when active Ras is absent. Upon release of the RBD and CRD, Raf undergoes an open conformation, exposing the dimerization surface of the kinase domain. However, in the absence of active Ras, this open conformation is not sustained. The binding of Raf to membrane-bound active Ras stabilizes the open conformation and facilitates Raf's localization to the membrane, ultimately promoting dimerization through side-to-side interaction between two kinase domains. With a high 14-3-3 population, Raf interacts with the 14-3-3 dimer, resulting in autoinhibited Raf with 14-3-3. Phosphorylation of Ser residues in the linker (Ser365 for B-Raf and Ser259 for Raf-1) and C-terminal tail (Ser729 for B-Raf and Ser621 for Raf-1) enhances the interaction between Raf and 14-3-3 proteins. In this state, phosphorylated Ser residues serve as anchor points for the association of the kinase domain with the 14-3-3 dimer. This interaction protects the dimerization surface. For Ras-free open Raf with 14-3-3, the released RBD can engage with GTP-bound Ras, promoting Raf dimerization. Phosphorylation of the Ser residue in the linker is required only for autoinhibition, whereas phosphorylation of the Ser residue in the C-terminal tail has a dual function in both kinase domain dimerization and autoinhibition.

well. Their differences lead to their differential membrane anchorage preferences, and altered interactions with varied stabilities with the same effectors.[198–201] Analysis of their dimer preferences demonstrates distinct behavior as well.[202] These point to differential distributions (propensities) of their conformational ensembles, which correlate with their altered preferred functions in different cell types. The Ras ensembles portray all states,[22,198,203] including the GTP and GDP bound conformations, effector bound states, membrane anchored active and inactive conformations, farnesylated, palmitoylated, phosphorylated, and ubiquitylated states, conformations harboring mutations, and transition states. Some conformations carry functions, others may not. All are allosterically modulated. Although all Ras isoforms have overlapping functions

and upon inhibition of one isoform can carry its tasks, they are optimized for specific cell types, suggesting distinct binding preferences by their respective conformations, with different isoforms exhibiting different signaling and biological functions. They may recruit different partners implicating different affinities or availabilities in the specific cell types that they populate or localize in. The interactions may also be GDP/GTP protein state dependent, although as we discussed above, GDP-bound conformations of strong driver mutations may trend toward the GTP-bound state. Within this framework, K-Ras splice isoforms K-Ras4A and K-Ras4B are of particular interest as they populate two states with lipid posttranslational modifications in their C-terminal hypervariable tails that mimic K-Ras4B, with only a farnesyl, and N-Ras, with a palmitoyl and
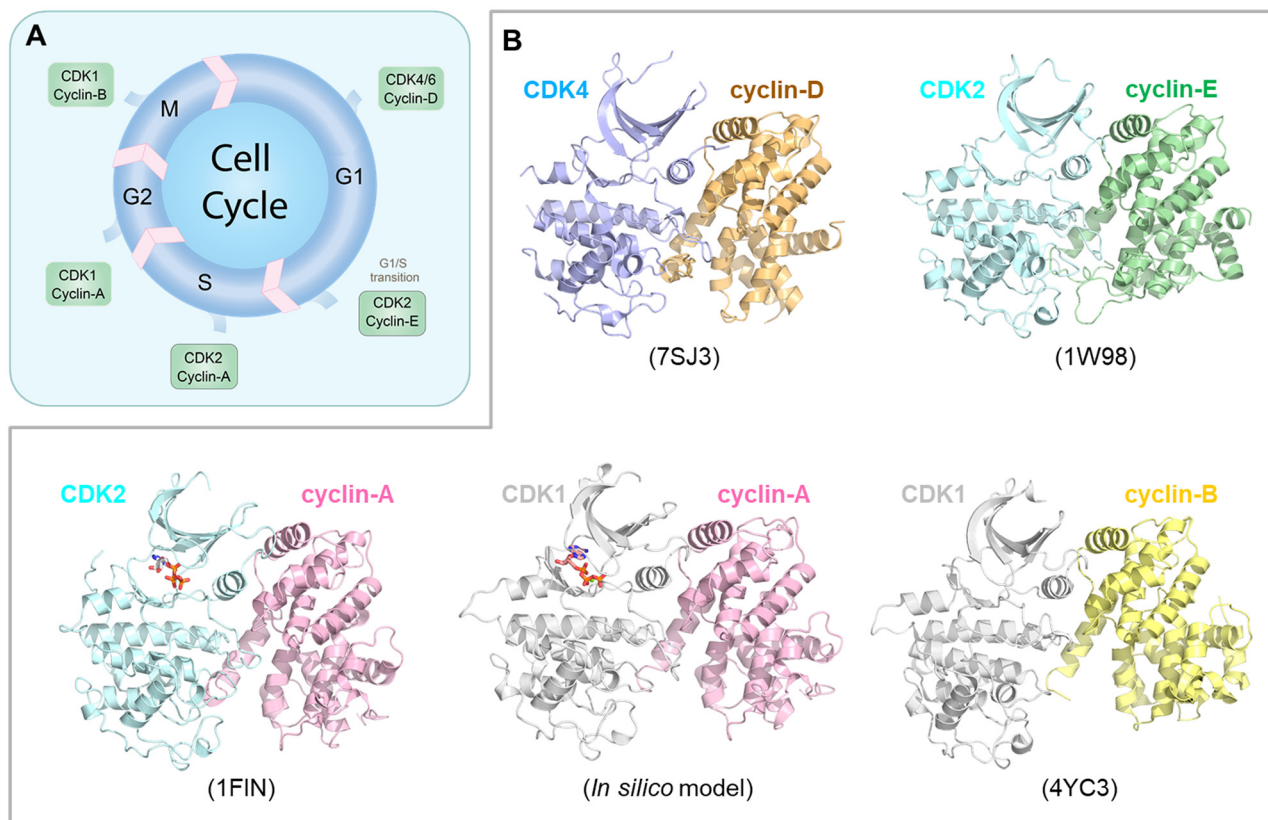
Fig. 7 Conformational diversity and regulation of CDKs in the cell cycle. (A) A schematic representation of the cell cycle, highlighting the involvement of various cyclin—CDK complexes at different phases (G1, S, G2, M). (B) Active conformations of the cyclin—CDK complexes participating in each stage of the cell cycle, with a focus on the structural similarities and subtle differences among them. These structural differences are crucial as they dictate the specific roles and regulatory functions of the complexes. Annotations include PDB codes for the crystal structures of the CDK complexes shown. In the absence of a crystal structure for the cyclin-A—CDK1 complex, an *in silico* model was constructed based on the active conformation of CDK1 and cyclin-A derived from the CDK2 complex. The figure also suggests the adaptability of CDKs; for example, when cyclin-E—CDK2 is unavailable for the G1/S transition, CDK1 can take over this role. Similarly, cyclin-B—CDK2 can substitute for CDK1 during the G2/M transition under certain conditions. The figure underscores the importance of structural variations and dynamic interactions in the fine-tuning of cell cycle regulation through cyclin—CDK complexes.

farnesyl.[198,203] The C-terminal of K-Ras4A is positively charged, in between the more highly positively charged K-Ras4B and the lesser charged N-Ras. This suggest that in its K-Ras4B-like conformation, K-Ras4A can be linked with K-Ras4B cancers, such as pancreatic ductal adenocarcinoma, colorectal, and lung cancers. In its N-Ras-like state it may be associated with melanoma, an N-Ras cancer. Recently, stable isotope labeling with amino acids in cell culture and affinity-purification mass spectrometry observed differences between K-Ras4A and K-Ras4B, which may explain some of the functional differences,[85] with v-ATPase a2 and eIF2Bδ interacting with only K-Ras4B. Especially of interest, K-Ras4A[G12D] binds Raf-1 stronger than K-Ras4B, reminiscent of the Rap1 inclination discussed above. We expect differential conformational trends of K-Ras4A[G12D] and K-Ras4B[G12D].

In another example, CDKs in the cell cycle are also similar and expected to share ensembles albeit with different propensities and distributions[204–206] (Fig. 7A). Especially, even though there are multiple CDKs, a single CDK is responsible for both G1/S and G2/M transitions.[207] Cyclin-E—CDK2 is the primary complex responsible for leading the cells through the G1/S transition stage (Fig. 7B), although recently, this "fixed point" estimate, which assumes that further cell cycle commitment ceases as soon as the mitogen signaling stimulus is removed, has been challenged.[208] However, when unavailable, CDK1 can undertake this role. Similarly, if its level is too low, CDK1 can be substituted by cyclin-B—CDK2 complexes in the G2/M checkpoint transition allowing cell cycle progression. Finally, sufficiently high hurdles in physiological time scales can constitute translational barriers with kinetically trapped states in synonymous single-nucleotide polymorphism. The translational pausing observed in the *MDR1* (multidrug resistance 1) gene can lead to alternative folded structures which are functionally distinct.[209–211] Eventually, the time scale of the altered conformation depends on the barrier height and relative stability. Recent examples concern type III chloramphenicol acetyltransferase, D-alanine-D-alanine ligase B and dihydrofolate reductase.[212]

Conclusions

Dynamic, interconverting, protein conformational ensembles sustain life. Rigid protein crystal structure snapshots do not.

Despite the overwhelming support for the need for conformational ensembles to understand function, still not all in the community accede to its veracity. The view that the change of a protein structure is *induced* by steric clashes, and electrostatic repulsion, which physically dislodge an impeding protein component is incompatible with a physics-based outlook. The concept underscored here is of a relationship between molecular structure and potential energy, where structures of conformers are related to their energy, and therefore to their relative stabilities.[213] This view explains that protein ensembles consist of all possible conformations with their populations depending on their relative energies. The partner protein selects the conformer whose shape and chemistry fit it best. Binding can still result in certain energetic frustration of local interactions.[121] Minimal local frustration indicates stable folded molecule; higher local frustration can point to functionally relevant regions where binding can promote allosteric signal that relieves it. Relieving the energetic frustration optimizes the interaction. Evolution exploited the ensemble by using the conformational ensemble for function. In our examples above, evolution has toyed with myristoyl to flip Abl conformations; in the case of K-Ras oncogenic mutations, the most aggressive K-Ras^{G12V} shifts the ensemble to the active state even when GDP-bound; in PI3K, an activated receptor binding shifts the ensemble to the active state, relieving the autoinhibition. And splicing isoforms preferentially bind partners to optimize function as in the case of K-Ras4A which favors Raf-1 whereas K-Ras4B prefers B-Raf, interestingly mimicking Rap1A, which favors B-Raf, over Raf-1. The C-terminal of Rap1A is strongly positively charged, resembling K-Ras4B. Rap1B's is neutral, resembling H-Ras and N-Ras.[86]

Here, we underscore conformational propensities. These determine protein function and cell activity. The relative number of active conformations, or molecules, decides the protein functional state: active or inactive. Together with expression level, they also determine signaling strength. Signaling strength decides cell activity. Exactly how to experimentally measure signal strength to establish cell activity is still enigmatic. Yet, this is vital as conformational propensities and the ensuing signaling strength can establish cell proliferation and forecast the emergence of drug resistance.

Author contributions

R. Nussinov, H. Jang: concept and original version. R. Nussinov: writing – original draft and supervision. Y. Liu, W. Zhang, H. Jang: visualization. R. Nussinov, Y. Liu, W. Zhang, H. Jang; writing – review and editing.

Conflicts of interest

There are no conflicts to declare.

Acknowledgements

Notes and references

1 J. N. Onuchic, Z. Luthey-Schulten and P. G. Wolynes, *Annu. Rev. Phys. Chem.*, 1997, **48**, 545–600.

2 H. Frauenfelder, S. G. Sligar and P. G. Wolynes, *Science*, 1991, **254**, 1598–1603.

3 F. Mallamace, C. Corsaro, D. Mallamace, S. Vasi, C. Vasi, P. Baglioni, S. V. Buldyrev, S. H. Chen and H. E. Stanley, *Proc. Natl. Acad. Sci. U. S. A.*, 2016, **113**, 3159–3163.

4 K. Roder and D. J. Wales, *Front. Mol. Biosci.*, 2022, **9**, 820792.

5 R. Nussinov and P. G. Wolynes, *Phys. Chem. Chem. Phys.*, 2014, **16**, 6321–6322.

6 K. Roder, J. A. Joseph, B. E. Husic and D. J. Wales, *Adv. Theor. Simul.*, 2019, **2**, 1800175.

7 S. Neelamraju, D. J. Wales and S. Gosavi, *Curr. Opin. Struct. Biol.*, 2020, **64**, 145–151.

8 S. H. Chen and R. Elber, *Phys. Chem. Chem. Phys.*, 2014, **16**, 6407–6421.

9 G. Wei, W. Xi, R. Nussinov and B. Ma, *Chem. Rev.*, 2016, **116**, 6516–6551.

10 P. Biswas, J. Zou and J. G. Saven, *J. Chem. Phys.*, 2005, **123**, 154908.

11 H. Nymeyer, N. D. Socci and J. N. Onuchic, *Proc. Natl. Acad. Sci. U. S. A.*, 2000, **97**, 634–639.

12 R. Nussinov, *Chem. Rev.*, 2016, **116**, 6263–6266.

13 A. M. Ruvinsky, T. Kirys, A. V. Tuzikov and I. A. Vakser, *Protein Sci.*, 2013, **22**, 734–744.

14 M. N. Sanches, K. Knapp, A. B. Oliveira, Jr., P. G. Wolynes, J. N. Onuchic and V. B. P. Leite, *J. Phys. Chem. B*, 2022, **126**, 93–99.

15 A. J. Wand, *Struct. Dyn.*, 2023, **10**, 020901.

16 J. Juarez-Jimenez, A. A. Gupta, G. Karunanithy, A. Mey, C. Georgiou, H. Ioannidis, A. De Simone, P. N. Barlow, A. N. Hulme, M. D. Walkinshaw, A. J. Baldwin and J. Michel, *Chem. Sci.*, 2020, **11**, 2670–2680.

17 J. Ding, Y. T. Lee, Y. Bhandari, C. D. Schwieters, L. Fan, P. Yu, S. G. Tarosov, J. R. Stagno, B. Ma, R. Nussinov, A. Rein, J. Zhang and Y. X. Wang, *Nat. Commun.*, 2023, **14**, 714.

18 R. Nussinov, M. Zhang, Y. Liu and H. Jang, *J. Phys. Chem. B*, 2022, **126**, 6372–6383.

19 B. Ma, G. Bai, R. Nussinov, J. Ding and Y. X. Wang, *J. Phys. Chem. B*, 2021, **125**, 2589–2596.

20 H. Jang, A. Banerjee, K. Marcus, L. Makowski, C. Mattos, V. Gaponenko and R. Nussinov, *Structure*, 2019, **27**, 1647–1659e1644.

21 R. Nussinov, C. J. Tsai and H. Jang, *PLoS Comput. Biol.*, 2019, **15**, e1006648.

22 S. Lu, H. Jang, S. Muratcioglu, A. Gursoy, O. Keskin, R. Nussinov and J. Zhang, *Chem. Rev.*, 2016, **116**, 6607–6665.

23 F. Yabukarski, T. Doukov, M. M. Pinney, J. T. Biel, J. S. Fraser and D. Herschlag, *Sci. Adv.*, 2022, **8**, eabn7738.

24 F. Yabukarski, J. T. Biel, M. M. Pinney, T. Doukov, A. S. Powers, J. S. Fraser and D. Herschlag, *Proc. Natl. Acad. Sci. U. S. A.*, 2020, **117**, 33204–33215.

25 M. I. Freiberger, P. G. Wolynes, D. U. Ferreiro and M. Fuxreiter, *J. Phys. Chem. B*, 2021, **125**, 2513–2520.

26 E. Karlsson, E. Andersson, J. Dogan, S. Gianni, P. Jemth and C. Camilloni, *J. Biol. Chem.*, 2019, **294**, 1230–1239.

27 N. Teruel, O. Mailhot and R. J. Najmanovich, *PLoS Comput. Biol.*, 2021, **17**, e1009286.

28 A. Nicolai, P. Delarue and P. Senet, *PLoS Comput. Biol.*, 2013, **9**, e1003379.

29 C. Draper-Joyce and S. G. B. Furness, *ACS Pharmacol. Transl. Sci.*, 2019, **2**, 285–290.

30 A. Pandini and A. Fornili, *J. Chem. Theory Comput.*, 2016, **12**, 1368–1379.

31 Y. Li and H. Gong, *J. Chem. Theory Comput.*, 2022, **18**, 4529–4543.

32 C. Kohler, G. Carlstrom, A. Gunnarsson, U. Weininger, S. Tangefjord, V. Ullah, M. Lepisto, U. Karlsson, T. Papavoine, K. Edman and M. Akke, *Sci. Adv.*, 2020, **6**, eabb5277.

33 Y. T. Lee, E. C. Glazer, R. F. Wilson, C. D. Stout and D. B. Goodin, *Biochemistry*, 2011, **50**, 693–703.

34 P. Grudzien, H. Jang, N. Leschinsky, R. Nussinov and V. Gaponenko, *J. Mol. Biol.*, 2022, **434**, 167695.

35 R. C. Maloney, M. Zhang, Y. Liu, H. Jang and R. Nussinov, *Cell. Mol. Life Sci.*, 2022, **79**, 281.

36 L. Zhang, M. Li and Z. Liu, *PLoS Comput. Biol.*, 2018, **14**, e1006393.

37 H. Abdelkarim, N. Leschinsky, H. Jang, A. Banerjee, R. Nussinov and V. Gaponenko, *Curr. Opin. Struct. Biol.*, 2021, **71**, 164–170.

38 M. Zhang, H. Jang and R. Nussinov, *Cancer Res.*, 2021, **81**, 237–247.

39 Q. Huang, P. Song, Y. Chen, Z. Liu and L. Lai, *J. Phys. Chem. Lett.*, 2021, **12**, 5404–5412.

40 J. Wang, A. Jain, L. R. McDonald, C. Gambogi, A. L. Lee and N. V. Dokholyan, *Nat. Commun.*, 2020, **11**, 3862.

41 R. Nussinov and C. J. Tsai, *Cell*, 2013, **153**, 293–305.

42 T. Haliloglu, A. Hacisuleyman and B. Erman, *Bioinformatics*, 2022, **38**, 3590–3599.

43 C. Stark, T. Bautista-Leung, J. Siegfried and D. Herschlag, *eLife*, 2022, **11**, e72884.

44 M. M. Pinney, D. A. Mokhtari, E. Akiva, F. Yabukarski, D. M. Sanchez, R. Liang, T. Doukov, T. J. Martinez, P. C. Babbitt and D. Herschlag, *Science*, 2021, **371**, eaay2784.

45 M. Zhang, R. Maloney, Y. Liu, H. Jang and R. Nussinov, *Cancer Commun.*, 2023, **43**, 405–408.

46 B. Ma, S. Kumar, C. J. Tsai, Z. Hu and R. Nussinov, *J. Theor. Biol.*, 2000, **203**, 383–397.

47 V. Galstyan and R. Phillips, *J. Phys. Chem. B*, 2019, **123**, 10990–11002.

48 T. R. Sosnick, *Protein Sci.*, 2008, **17**, 1308–1318.

49 S. J. Wodak, E. Paci, N. V. Dokholyan, I. N. Berezovsky, A. Horovitz, J. Li, V. J. Hilser, I. Bahar, J. Karanicolas, G. Stock, P. Hamm, R. H. Stote, J. Eberhardt, Y. Chebaro, A. Dejaegere, M. Cecchini, J. P. Changeux, P. G. Bolhuis, J. Vreede, P. Faccioli, S. Orioli, R. Ravasio, L. Yan, C. Brito, M. Wyart, P. Gkeka, I. Rivalta, G. Palermo, J. A. McCammon, J. Panecka-Hofman, R. C. Wade, A. Di Pizio, M. Y. Niv, R. Nussinov, C. J. Tsai, H. Jang, D. Padhorny, D. Kozakov and T. McLeish, *Structure*, 2019, **27**, 566–578.

50 V. Munoz and M. Cerminara, *Biochem. J.*, 2016, **473**, 2545–2559.

51 S. Kang, A. G. Bader and P. K. Vogt, *Proc. Natl. Acad. Sci. U. S. A.*, 2005, **102**, 802–807.

52 M. Sun, P. Hillmann, B. T. Hofmann, J. R. Hart and P. K. Vogt, *Proc. Natl. Acad. Sci. U. S. A.*, 2010, **107**, 15547–15552.

53 J. E. Burke, O. Perisic, G. R. Masson, O. Vadas and R. L. Williams, *Proc. Natl. Acad. Sci. U. S. A.*, 2012, **109**, 15259–15264.

54 R. Nussinov, M. Zhang, R. Maloney and H. Jang, *Expert Opin. Drug Discovery*, 2021, **16**, 823–828.

55 S. Du, S. A. Wankowicz, F. Yabukarski, T. Doukov, D. Herschlag and J. S. Fraser, *bioRxiv*, 2023, DOI: **10.1101/2023.05.05.539620**.

56 C. Di Pietrantonio, A. Pandey, J. Gould, A. Hasabnis and R. S. Prosser, *Methods Enzymol.*, 2019, **615**, 103–130.

57 A. N. Naganathan, R. Dani, S. Gopi, A. Aranganathan and A. Narayan, *J. Mol. Biol.*, 2021, **433**, 167325.

58 K. Lindorff-Larsen and J. Ferkinghoff-Borg, *PLoS One*, 2009, **4**, e4203.

59 S. Kumar, B. Ma, C. J. Tsai, N. Sinha and R. Nussinov, *Protein Sci.*, 2000, **9**, 10–19.

60 C. J. Tsai, S. Kumar, B. Ma and R. Nussinov, *Protein Sci.*, 1999, **8**, 1181–1190.

61 C. J. Tsai, B. Ma and R. Nussinov, *Proc. Natl. Acad. Sci. U. S. A.*, 1999, **96**, 9970–9972.

62 B. Ma, S. Kumar, C. J. Tsai and R. Nussinov, *Protein Eng.*, 1999, **12**, 713–720.

63 O. Farc and V. Cristea, *Exp. Ther. Med.*, 2021, **21**, 96.

64 A. Ma'ayan, *J. R. Soc., Interface*, 2017, **14**, 20170391.

65 K. Ingram, S. C. Samson, R. Zewdu, R. G. Zitnay, E. L. Snyder and M. C. Mendoza, *Oncogene*, 2022, **41**, 293–300.

66 R. Mukherjee, K. G. Vanaja, J. A. Boyer, S. Gadal, H. Solomon, S. Chandarlapaty, A. Levchenko and N. Rosen, *Mol. Cell*, 2021, **81**, 708–723e705.

67 J. Stebbing, L. C. Lit, H. Zhang, R. S. Darrington, O. Melaiu, B. Rudraraju and G. Giamas, *Oncogene*, 2014, **33**, 939–953.

68 W. S. Chen, Y. Liang, M. Zong, J. J. Liu, K. Kaneko, K. L. Hanley, K. Zhang and G. S. Feng, *Cell Rep.*, 2021, **37**, 109974.

69 L. Guo, K. Zhu, M. Pargett, A. Contreras, P. Tsai, Q. Qing, W. Losert, J. Albeck and M. Zhao, *iScience*, 2021, **24**, 103240.

70 R. Nussinov, *Phys. Biol.*, 2013, **10**, 045004.

© 2023 The Author(s). Published by the Royal Society of Chemistry

RSC Chem. Biol., 2023, **4**, 850–864 | **861**

71 L. Wakefield, S. Agarwal and K. Tanner, *Cell*, 2023, **186**, 1792–1813.

72 D. S. W. Lee, N. S. Wingreen and C. P. Brangwynne, *Nat. Phys.*, 2021, **17**, 531–538.

73 A. L. S. Cruz, N. Carrossini, L. K. Teixeira, L. F. Ribeiro-Pinto, P. T. Bozza and J. P. B. Viola, *Mol. Cell. Biol.*, 2019, **39**, e00374–18.

74 C. A. Weber and C. Zechner, *Phys. Today*, 2021, **74**, 38–43.

75 J. Liu and R. Nussinov, *PLoS Comput. Biol.*, 2016, **12**, e1004966.

76 M. Leander, Y. Yuan, A. Meger, Q. Cui and S. Raman, *Proc. Natl. Acad. Sci. U. S. A.*, 2020, **117**, 25445–25454.

77 P. Campitelli, T. Modi, S. Kumar and S. B. Ozkan, *Annu. Rev. Biophys.*, 2020, **49**, 267–288.

78 G. M. Verkhivker and L. Di Paola, *J. Phys. Chem. B*, 2021, **125**, 850–873.

79 G. M. Verkhivker, *Curr. Opin. Struct. Biol.*, 2021, **71**, 71–78.

80 Y. Yuan, J. Deng and Q. Cui, *J. Am. Chem. Soc.*, 2022, **144**, 10870–10887.

81 M. Leander, Z. Liu, Q. Cui and S. Raman, *eLife*, 2022, **11**, e79932.

82 A. Dayananda, T. S. H. Dennison, H. Y. Y. Fonseka, M. S. Avestan, Q. Wang, R. Tehver and G. Stan, *J. Chem. Phys.*, 2023, **158**, 125101.

83 S. Dey and H. X. Zhou, *J. Chem. Phys.*, 2023, **158**, 091105.

84 R. Nussinov, H. Jang, G. Nir, C. J. Tsai and F. Cheng, *Signal Transduction Targeted Ther.*, 2021, **6**, 3.

85 X. Zhang, J. Cao, S. P. Miller, H. Jing and H. Lin, *ACS Cent. Sci.*, 2018, **4**, 71–80.

86 R. Nussinov, H. Jang, M. Zhang, C. J. Tsai and A. A. Sablina, *Trends Cancer*, 2020, **6**, 369–379.

87 R. Nussinov, C. J. Tsai and H. Jang, *Adv. Exp. Med. Biol.*, 2019, **1163**, 25–43.

88 K. Gunasekaran, B. Ma and R. Nussinov, *Proteins*, 2004, **57**, 433–443.

89 R. Nussinov, M. Zhang, R. Maloney, Y. Liu, C. J. Tsai and H. Jang, *J. Mol. Biol.*, 2022, **434**, 167569.

90 C. J. Tsai and R. Nussinov, *PLoS Comput. Biol.*, 2014, **10**, e1003394.

91 A. del Sol, C. J. Tsai, B. Ma and R. Nussinov, *Structure*, 2009, **17**, 1042–1050.

92 Q. Cui and M. Karplus, *Protein Sci.*, 2008, **17**, 1295–1307.

93 J. P. Changeux and A. Christopoulos, *Cell*, 2016, **166**, 1084–1102.

94 A. Chatzigoulas and Z. Cournia, *Wiley Interdiscip. Rev.: Comput. Mol. Sci.*, 2021, **11**, e1529.

95 G. Kar, O. Keskin, A. Gursoy and R. Nussinov, *Curr. Opin. Pharmacol.*, 2010, **10**, 715–722.

96 V. J. Hilser, J. O. Wrabl and H. N. Motlagh, *Annu. Rev. Biophys.*, 2012, **41**, 585–609.

97 J. P. Changeux, *Annu. Rev. Biophys.*, 2012, **41**, 103–133.

98 S. Schann, S. Mayer, C. Franchet, M. Frauli, E. Steinberg, M. Thomas, L. Baron and P. Neuville, *J. Med. Chem.*, 2010, **53**, 8775–8779.

99 T. W. Schwartz and B. Holst, *Trends Pharmacol. Sci.*, 2007, **28**, 366–373.

100 C. J. Wenthur, P. R. Gentry, T. P. Mathews and C. W. Lindsley, *Annu. Rev. Pharmacol. Toxicol.*, 2014, **54**, 165–184.

101 Z. Fang, C. Grutter and D. Rauh, *ACS Chem. Biol.*, 2013, **8**, 58–70.

102 F. Quaglia, T. Lazar, A. Hatos, P. Tompa, D. Piovesan and S. C. E. Tosatto, *Curr. Protoc.*, 2021, **1**, e192.

103 A. Bah and J. D. Forman-Kay, *J. Biol. Chem.*, 2016, **291**, 6696–6705.

104 F. Jin and F. Grater, *PLoS Comput. Biol.*, 2021, **17**, e1008939.

105 R. Nussinov, C. J. Tsai, F. Xin and P. Radivojac, *Trends Biochem. Sci.*, 2012, **37**, 447–455.

106 G. Stetz, A. Tse and G. M. Verkhivker, *Sci. Rep.*, 2018, **8**, 6899.

107 A. S. Venne, L. Kollipara and R. P. Zahedi, *Proteomics*, 2014, **14**, 513–524.

108 B. C. Lechtenberg, M. P. Gehring, T. P. Light, C. R. Horne, M. W. Matsumoto, K. Hristova and E. B. Pasquale, *Nat. Commun.*, 2021, **12**, 7047.

109 L. Alaalm, J. L. Crunden, M. Butcher, U. Obst, R. Whealy, C. E. Williamson, H. E. O'Brien, C. Schaffitzel, G. Ramage, J. Spencer and S. Diezmann, *Front. Cell. Infect. Microbiol.*, 2021, **11**, 637836.

110 N. Sostaric and V. van Noort, *PLoS Comput. Biol.*, 2021, **17**, e1008988.

111 H. Zhang, J. He, G. Hu, F. Zhu, H. Jiang, J. Gao, H. Zhou, H. Lin, Y. Wang, K. Chen, F. Meng, M. Hao, K. Zhao, C. Luo and Z. Liang, *J. Med. Chem.*, 2021, **64**, 15111–15125.

112 H. F. Liu and R. Liu, *Briefings Bioinf.*, 2020, **21**, 609–620.

113 R. Nussinov and C. J. Tsai, *Curr. Pharm. Des.*, 2012, **18**, 1311–1316.

114 J. A. Byun, B. VanSchouwen, M. Akimoto and G. Melacini, *Comput. Struct. Biotechnol. J.*, 2020, **18**, 3803–3818.

115 J. R. Wagner, C. T. Lee, J. D. Durrant, R. D. Malmstrom, V. A. Feher and R. E. Amaro, *Chem. Rev.*, 2016, **116**, 6370–6390.

116 A. K. Gupta, X. Wang, C. V. Pagba, P. Prakash, S. Sarkar-Banerjee, J. Putkey and A. A. Gorfe, *Chem. Biol. Drug Des.*, 2019, **94**, 1441–1456.

117 B. Musafia and H. Senderowitz, *Expert Opin. Drug Discovery*, 2010, **5**, 943–959.

118 F. Marchetti, E. Moroni, A. Pandini and G. Colombo, *J. Phys. Chem. Lett.*, 2021, **12**, 3724–3732.

119 N. Greives and H. X. Zhou, *Proc. Natl. Acad. Sci. U. S. A.*, 2014, **111**, 10197–10202.

120 J. W. Biddle, R. Martinez-Corral, F. Wong and J. Gunawardena, *eLife*, 2021, **10**, e65498.

121 A. B. Guzovsky, N. P. Schafer, P. G. Wolynes and D. U. Ferreiro, *Methods Mol. Biol.*, 2022, **2376**, 387–398.

122 R. G. Parra, N. P. Schafer, L. G. Radusky, M. Y. Tsai, A. B. Guzovsky, P. G. Wolynes and D. U. Ferreiro, *Nucleic Acids Res.*, 2016, **44**, W356–360.

123 S. Gianni, M. I. Freiberger, P. Jemth, D. U. Ferreiro, P. G. Wolynes and M. Fuxreiter, *Acc. Chem. Res.*, 2021, **54**, 1251–1259.

124 A. Olivera and J. M. Lopez-Novoa, *Br. J. Pharmacol.*, 1992, **107**, 341–346.

125 L. Ponzoni and I. Bahar, *Proc. Natl. Acad. Sci. U. S. A.*, 2018, **115**, 4164–4169.

126 P. Csermely, T. Korcsmaros, H. J. Kiss, G. London and R. Nussinov, *Pharmacol. Ther.*, 2013, **138**, 333–408.

127 X. Ma, H. Meng and L. Lai, *J. Chem. Inf. Model.*, 2016, **56**, 1725–1733.

128 L. Astl and G. M. Verkhivker, *J. Chem. Inf. Model.*, 2020, **60**, 1614–1631.

129 L. M. Pietrek, L. S. Stelzl and G. Hummer, *Curr. Opin. Struct. Biol.*, 2023, **78**, 102501.

130 P. E. Wright and H. J. Dyson, *J. Mol. Biol.*, 1999, **293**, 321–331.

131 G. W. Gomes, M. Krzeminski, A. Namini, E. W. Martin, T. Mittag, T. Head-Gordon, J. D. Forman-Kay and C. C. Gradinaru, *J. Am. Chem. Soc.*, 2020, **142**, 15697–15710.

132 P. Kulkarni, S. Bhattacharya, S. Achuthan, A. Behal, M. K. Jolly, S. Kotnala, A. Mohanty, G. Rangarajan, R. Salgia and V. Uversky, *Chem. Rev.*, 2022, **122**, 6614–6633.

133 C. Gao, C. Ma, H. Wang, H. Zhong, J. Zang, R. Zhong, F. He and D. Yang, *Sci. Rep.*, 2021, **11**, 2985.

134 N. Rangarajan, P. Kulkarni and S. Hannenhalli, *PLoS One*, 2015, **10**, e0126729.

135 M. K. Yoon, D. M. Mitrea, L. Ou and R. W. Kriwacki, *Biochem. Soc. Trans.*, 2012, **40**, 981–988.

136 V. N. Uversky, *Front. Phys.*, 2019, **7**, 10.

137 Z. Peng, J. Yan, X. Fan, M. J. Mizianty, B. Xue, K. Wang, G. Hu, V. N. Uversky and L. Kurgan, *Cell. Mol. Life Sci.*, 2015, **72**, 137–151.

138 J. J. Ward, J. S. Sodhi, L. J. McGuffin, B. F. Buxton and D. T. Jones, *J. Mol. Biol.*, 2004, **337**, 635–645.

139 H. J. Dyson, *Q. Rev. Biophys.*, 2011, **44**, 467–518.

140 P. Radivojac, L. M. Iakoucheva, C. J. Oldfield, Z. Obradovic, V. N. Uversky and A. K. Dunker, *Biophys. J.*, 2007, **92**, 1439–1456.

141 R. Nussinov, C. J. Tsai and H. Jang, *Front. Oncol.*, 2019, **9**, 1231.

142 D. D. Boehr, R. Nussinov and P. E. Wright, *Nat. Chem. Biol.*, 2009, **5**, 789–796.

143 H. N. Motlagh, J. O. Wrabl, J. Li and V. J. Hilser, *Nature*, 2014, **508**, 331–339.

144 Y. Liu, M. Zhang, C. J. Tsai, H. Jang and R. Nussinov, *Comput. Struct. Biotechnol. J.*, 2022, **20**, 4257–4270.

145 B. Nagar, O. Hantschel, M. A. Young, K. Scheffzek, D. Veach, W. Bornmann, B. Clarkson, G. Superti-Furga and J. Kuriyan, *Cell*, 2003, **112**, 859–871.

146 T. Saleh, P. Rossi and C. G. Kalodimos, *Nat. Struct. Mol. Biol.*, 2017, **24**, 893–901.

147 O. Hantschel, B. Nagar, S. Guettler, J. Kretzschmar, K. Dorey, J. Kuriyan and G. Superti-Furga, *Cell*, 2003, **112**, 845–857.

148 T. Xie, T. Saleh, P. Rossi and C. G. Kalodimos, *Science*, 2020, **370**, eabc2754.

149 K. M. Smith, R. Yacobi and R. A. Van Etten, *Mol. Cell*, 2003, **12**, 27–37.

150 F. Grebien, O. Hantschel, J. Wojcik, I. Kaupe, B. Kovacic, A. M. Wyrzucki, G. D. Gish, S. Cerny-Reiterer, A. Koide,

H. Beug, T. Pawson, P. Valent, S. Koide and G. Superti-Furga, *Cell*, 2011, **147**, 306–319.

151 S. Panjarian, R. E. Iacob, S. Chen, T. E. Wales, J. R. Engen and T. E. Smithgall, *J. Biol. Chem.*, 2013, **288**, 6116–6129.

152 M. L. Martin-Fernandez, D. T. Clarke, S. K. Roberts, L. C. Zanetti-Domingues and F. L. Gervasio, *Cells*, 2019, **8**, 316.

153 S. Chen, S. Brier, T. E. Smithgall and J. R. Engen, *Protein Sci.*, 2007, **16**, 572–581.

154 O. Hantschel and G. Superti-Furga, *Nat. Rev. Mol. Cell Biol.*, 2004, **5**, 33–44.

155 F. Al-Mulla, E. J. Milner-White, J. J. Going and G. D. Birnie, *J. Pathol.*, 1999, **187**, 433–438.

156 N. T. Ihle, L. A. Byers, E. S. Kim, P. Saintigny, J. J. Lee, G. R. Blumenschein, A. Tsao, S. Liu, J. E. Larsen, J. Wang, L. Diao, K. R. Coombes, L. Chen, S. Zhang, M. F. Abdelmelek, X. Tang, V. Papadimitrakopoulou, J. D. Minna, S. M. Lippman, W. K. Hong, R. S. Herbst, I. I. Wistuba, J. V. Heymach and G. Powis, *J. Natl. Cancer Inst.*, 2012, **104**, 228–239.

157 J. C. Hunter, A. Manandhar, M. A. Carrasco, D. Gurbani, S. Gondi and K. D. Westover, *Mol. Cancer Res.*, 2015, **13**, 1325–1335.

158 M. V. Cespedes, F. J. Sancho, S. Guerrero, M. Parreno, I. Casanova, M. A. Pavon, E. Marcuello, M. Trias, M. Cascante, G. Capella and R. Mangues, *Carcinogenesis*, 2006, **27**, 2190–2200.

159 M. C. Garassino, M. Marabese, P. Rusconi, E. Rulli, O. Martelli, G. Farina, A. Scanni and M. Broggini, *Ann. Oncol.*, 2011, **22**, 235–237.

160 A. Wittinghofer, K. Scheffzek and M. R. Ahmadian, *FEBS Lett.*, 1997, **410**, 63–67.

161 Y. Wang, D. Ji, C. Lei, Y. Chen, Y. Qiu, X. Li, M. Li, D. Ni, J. Pu, J. Zhang, Q. Fu, Y. Liu and S. Lu, *Comput. Struct. Biotechnol. J.*, 2021, **19**, 1184–1199.

162 S. Lu, H. Jang, R. Nussinov and J. Zhang, *Sci. Rep.*, 2016, **6**, 21949.

163 H. Jang, J. Chen, L. M. Iakoucheva and R. Nussinov, *bioRxiv*, 2023, DOI: 10.1101/2023.01.26.525746.

164 R. Nussinov, C. J. Tsai and H. Jang, *Cancer Res.*, 2022, **82**, 4114–4123.

165 M. Geyer and A. Wittinghofer, *Curr. Opin. Struct. Biol.*, 1997, **7**, 786–792.

166 E. M. Terrell and D. K. Morrison, *Cold Spring Harbor Perspect. Med.*, 2019, **9**, a033746.

167 M. Zhang, H. Jang and R. Nussinov, *Chem. Sci.*, 2019, **10**, 3671–3680.

168 D. A. Fruman, H. Chiu, B. D. Hopkins, S. Bagrodia, L. C. Cantley and R. T. Abraham, *Cell*, 2017, **170**, 605–635.

169 M. S. Lawrence, P. Stojanov, C. H. Mermel, J. T. Robinson, L. A. Garraway, T. R. Golub, M. Meyerson, S. B. Gabriel, E. S. Lander and G. Getz, *Nature*, 2014, **505**, 495–501.

170 L. Stephens, R. Williams and P. Hawkins, *Curr. Opin. Pharmacol.*, 2005, **5**, 357–365.

171 L. M. Thorpe, H. Yuzugullu and J. J. Zhao, *Nat. Rev. Cancer*, 2015, **15**, 7–24.

© 2023 The Author(s). Published by the Royal Society of Chemistry

RSC Chem. Biol., 2023, **4**, 850–864 | **863**

172 R. Williams, A. Berndt, S. Miller, W. C. Hon and X. Zhang, *Biochem. Soc. Trans.*, 2009, **37**, 615–626.

173 C. H. Huang, D. Mandelker, O. Schmidt-Kittler, Y. Samuels, V. E. Velculescu, K. W. Kinzler, B. Vogelstein, S. B. Gabelli and L. M. Amzel, *Science*, 2007, **318**, 1744–1748.

174 M. S. Miller, O. Schmidt-Kittler, D. M. Bolduc, E. T. Brower, D. Chaves-Moreira, M. Allaire, K. W. Kinzler, I. G. Jennings, P. E. Thompson, P. A. Cole, L. M. Amzel, B. Vogelstein and S. B. Gabelli, *Oncotarget*, 2014, **5**, 5198–5208.

175 D. A. Fruman and C. Rommel, *Nat. Rev. Drug Discovery*, 2014, **13**, 140–156.

176 R. Nussinov, G. Wang, C. J. Tsai, H. Jang, S. Lu, A. Banerjee, J. Zhang and V. Gaponenko, *Trends Cancer*, 2017, **3**, 214–224.

177 M. Zhang, H. Jang, V. Gaponenko and R. Nussinov, *Biophys. J.*, 2017, **113**, 1956–1967.

178 M. Zhang, H. Jang, Z. Li, D. B. Sacks and R. Nussinov, *Structure*, 2021, **29**, 768–777e762.

179 H. Chong and K. L. Guan, *J. Biol. Chem.*, 2003, **278**, 36269–36276.

180 C. Herrmann, G. Horn, M. Spaargaren and A. Wittinghofer, *J. Biol. Chem.*, 1996, **271**, 6794–6800.

181 H. Jang, M. Zhang and R. Nussinov, *Comput. Struct. Biotechnol. J.*, 2020, **18**, 737–748.

182 S. Li, H. Jang, J. Zhang and R. Nussinov, *Structure*, 2018, **26**, 513–525e512.

183 Z. L. Li, P. Prakash and M. Buck, *ACS Cent. Sci.*, 2018, **4**, 298–305.

184 T. Travers, C. A. Lopez, Q. N. Van, C. Neale, M. Tonelli, A. G. Stephen and S. Gnanakaran, *Sci. Rep.*, 2018, **8**, 8461.

185 T. Improta-Brears, S. Ghosh and R. M. Bell, *Mol. Cell. Biochem.*, 1999, **198**, 171–178.

186 N. R. Michaud, J. R. Fabian, K. D. Mathes and D. K. Morrison, *Mol. Cell. Biol.*, 1995, **15**, 3390–3397.

187 G. Tzivion, Z. Luo and J. Avruch, *Nature*, 1998, **394**, 88–92.

188 A. J. Muslin, J. W. Tanner, P. M. Allen and A. S. Shaw, *Cell*, 1996, **84**, 889–897.

189 C. Rommel, G. Radziwill, J. Lovric, J. Noeldeke, T. Heinicke, D. Jones, A. Aitken and K. Moelling, *Oncogene*, 1996, **12**, 609–619.

190 H. Lavoie and M. Therrien, *Nat. Rev. Mol. Cell Biol.*, 2015, **16**, 281–298.

191 A. S. Dhillon, S. Meikle, Z. Yazici, M. Eulitz and W. Kolch, *EMBO J.*, 2002, **21**, 64–71.

192 D. Abraham, K. Podar, M. Pacher, M. Kubicek, N. Welzel, B. A. Hemmings, S. M. Dilworth, H. Mischak, W. Kolch and M. Baccarini, *J. Biol. Chem.*, 2000, **275**, 22300–22304.

193 M. Jaumot and J. F. Hancock, *Oncogene*, 2001, **20**, 3949–3958.

194 D. Matallanas, M. Birtwistle, D. Romano, A. Zebisch, J. Rauch, A. von Kriegsheim and W. Kolch, *Genes Cancer*, 2011, **2**, 232–260.

195 M. Zhang, H. Jang and R. Nussinov, *Phys. Chem. Chem. Phys.*, 2019, **21**, 12021–12028.

196 G. A. Hobbs, C. J. Der and K. L. Rossman, *J. Cell Sci.*, 2016, **129**, 1287–1292.

197 F. E. Hood, Y. M. Sahraoui, R. E. Jenkins and I. A. Prior, *Oncogene*, 2023, **42**, 1224–1232.

198 R. Nussinov, C. J. Tsai, M. Chakrabarti and H. Jang, *Cancer Res.*, 2016, **76**, 18–23.

199 A. Y. Volmar, H. Guterres, H. Zhou, D. Reid, S. Pavlopoulos, L. Makowski and C. Mattos, *Biophys. J.*, 2022, **121**, 3616–3629.

200 J. A. Parker, A. Y. Volmar, S. Pavlopoulos and C. Mattos, *Structure*, 2018, **26**, 810–820e814.

201 J. A. Parker and C. Mattos, *Cold Spring Harbor Perspect. Med.*, 2018, **8**, a031427.

202 H. Jang, S. Muratcioglu, A. Gursoy, O. Keskin and R. Nussinov, *Biochem. J.*, 2016, **473**, 1719–1732.

203 F. D. Tsai, M. S. Lopes, M. Zhou, H. Court, O. Ponce, J. J. Fiordalisi, J. J. Gierut, A. D. Cox, K. M. Haigis and M. R. Philips, *Proc. Natl. Acad. Sci. U. S. A.*, 2015, **112**, 779–784.

204 E. S. Knudsen, V. Kumarasamy, R. Nambiar, J. D. Pearson, P. Vail, H. Rosenheck, J. Wang, K. Eng, R. Bremner, D. Schramek, S. M. Rubin, A. L. Welm and A. K. Witkiewicz, *Cell Rep.*, 2022, **38**, 110448.

205 M. Barbiero, L. Cirillo, S. Veerapathiran, C. Coates, C. Ruffilli and J. Pines, *Open Biol.*, 2022, **12**, 220057.

206 M. Malumbres and M. Barbacid, *Nat. Rev. Cancer*, 2009, **9**, 153–166.

207 H. W. Lau, H. T. Ma, T. K. Yeung, M. Y. Tam, D. Zheng, S. K. Chu and R. Y. C. Poon, *Cell Rep.*, 2021, **37**, 109808.

208 R. F. Brooks, *Cell Div.*, 2023, **18**, 2.

209 C. J. Tsai, Z. E. Sauna, C. Kimchi-Sarfaty, S. V. Ambudkar, M. M. Gottesman and R. Nussinov, *J. Mol. Biol.*, 2008, **383**, 281–291.

210 C. Kimchi-Sarfaty, J. M. Oh, I. W. Kim, Z. E. Sauna, A. M. Calcagno, S. V. Ambudkar and M. M. Gottesman, *Science*, 2007, **315**, 525–528.

211 R. C. Hunt and C. Kimchi-Sarfaty, *N. Engl. J. Med.*, 2022, **387**, 753–756.

212 Y. Jiang, S. S. Neti, I. Sitarik, P. Pradhan, P. To, Y. Xia, S. D. Fried, S. J. Booker and E. P. O'Brien, *Nat. Chem.*, 2023, **15**, 308–318.

213 T. R. Weikl and F. Paul, *Protein Sci.*, 2014, **23**, 1508–1518.